

---

## **Chapter 2**

---

*Experimental: Materials and  
methods*

---

## 2.1. Introduction

This chapter portrays the methodologies adopted for synthesis, characterizations, and evaluation of the photocatalytic activity of as-prepared materials for the degradation of organic pollutants. All the chemicals and reagents employed in the studies were presented in tabular form below. The details of different characterization techniques viz. X-ray diffraction pattern (XRD), Transmission electron microscopy (TEM), X-ray photoelectron spectroscopy (XPS), ultra-violet spectroscopy (UV), ultra-violet diffused reflectance spectroscopy (UV-DRS) and photoluminescence (PL) studies with their fundamental and operating conditions have been discussed. Moreover, the chapter also describes the general procedure adopted for evaluating the photocatalytic activities of the CuWO<sub>4</sub>-based nanocomposite materials prepared in this thesis work.

## 2.2. Chemicals

Analytical-grade chemicals were procured from commercial sources and utilized without further purification. Table 2.1 tabulates the chemicals used in this thesis. Deionized double distilled water (DDDW) was utilized as a synthesis medium, and photocatalytic performances of prepared materials were also evaluated in the same medium.

**Table 2.1:** Names, chemical formula, molecular weights, manufacturer's name, and physical appearances of the reagents used.

<b>Sr. No.</b>	<b>Chemical name</b>	<b>Chemical formula</b>	<b>Molecular weight (g/mol)</b>	<b>Manufacturer</b>	<b>Physical Appearance</b>
1	Copper nitrate trihydrate	Cu(NO <sub>3</sub> ) <sub>2</sub> .3H <sub>2</sub> O	187.56	Merck	Blue Crystal

2	Sodium Tungstate dihydrate	$\text{Na}_2\text{WO}_4 \cdot 2\text{H}_2\text{O}$	329.86	Merck	White Crystals
3	Sodium bicarbonate	$\text{NaHCO}_3$	84.01	Merck	White powder
4	Sodium hydrogen phosphate	$\text{Na}_2\text{HPO}_4$	141.96	Sigma Aldrich	Yellowish powder
5	Trisodium Vanadate	$\text{Na}_3\text{VO}_4$	183.91		White Crystals
4	Tetracycline	$\text{C}_{22}\text{H}_{24}\text{N}_2\text{O}_8$	444.43	Sigma Aldrich	Light Yellow powder
5	Ciprofloxacin	$\text{C}_7\text{H}_{18}\text{FN}_3\text{O}_3$	331.34	Merck	White
6	Rhodamine B	$\text{C}_{28}\text{H}_{31}\text{ClN}_2\text{O}_3$	479.02	Merck	Reddish violet
7	Methyl orange	$\text{C}_{14}\text{H}_{14}\text{N}_3\text{NaO}_3\text{S}$	327.33	Molychem	Orange powder
8	Silver nitrate	$\text{AgNO}_3$	169.87	Merck	White crystal
9	Sodium Molybdate	$\text{Na}_2\text{MoO}_4 \cdot 2\text{H}_2\text{O}$	241.96	Merck	White crystal
10	Copper Acetate dihydrate	$\text{Cu}(\text{OAc})_2 \cdot 2\text{H}_2\text{O}$	249.68	Merck	Blue Crystal
11	Sodium hydroxide	$\text{NaOH}$	40.00	Merck	White Pellet
12	Polyvinylpyrrolidone (PVP)	$(\text{C}_6\text{H}_9\text{NO})_n$	176.12	Merck	White powder
13	Hydrochloric acid	$\text{HCl}$	36.46	Merck	Colourless liquid
14	para benzoquinone	$\text{C}_6\text{H}_4\text{O}_2$	108.09	Merck	Yellow Crystal
15	isopropyl alcohol	$\text{C}_3\text{H}_8\text{O}$	60.10	Merck	Colourless liquid

---

16	Potassium iodide	KI	166.00	Merck	White crystal
17	Acetonitrile	CH <sub>3</sub> CN	41.05	Merck	Colourless liquid

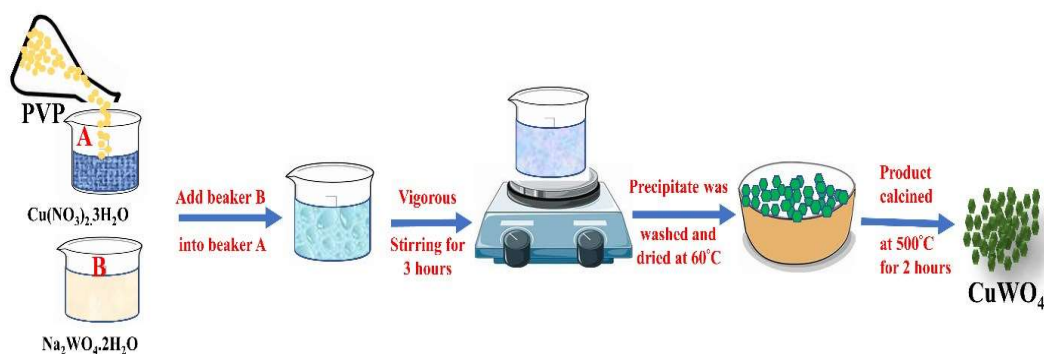
---

### **2.3. Sample preparation**

This thesis describes utilizing the co-precipitation method for the preparation of nanocomposites. The synthesis of CuWO<sub>4</sub> and Ag<sub>3</sub>PO<sub>4</sub>/CuWO<sub>4</sub> nanocomposite has been done by precipitation followed by calcination and a hydrothermal treatment method, respectively. A stainless-steel autoclave was utilized for the hydrothermal treatment. The synthesis procedure for CuWO<sub>4</sub> is discussed below, while the synthesis of AgI/CuWO<sub>4</sub>, Ag<sub>3</sub>PO<sub>4</sub>/CuWO<sub>4</sub>, Ag<sub>3</sub>VO<sub>4</sub>/CuWO<sub>4</sub>, and Ag<sub>2</sub>MoO<sub>4</sub>/CuWO<sub>4</sub> nanocomposite preparations was given in the sample preparation sections of respective chapters 3, 4, 5, and 6.

#### **3.2.1. Synthesis of CuWO<sub>4</sub>**

CuWO<sub>4</sub> was prepared by a precipitation method. The first step was the preparation of 20 ml each of 0.015M sodium tungstate and 0.015M copper nitrate aqueous solutions in separate beakers labelled A and B, respectively. A proper amount of PVP was then added to beaker B and stirred for 30 minutes. Next, the sodium tungstate solution was added to the contents in beaker B and sonicated for 60 minutes. The system was allowed to cool, and the obtained dark green precipitate was washed several times with DI water and ethanol. The final product was calcined at 500°C for 2 hours.



**Scheme 2.1:** Graphical representation of the synthesis of CuWO<sub>4</sub>

#### 2.4. Techniques used for materials characterization

This section describes the techniques used to characterize the prepared nanocomposites. The X-ray diffraction (XRD) technique was applied to identify the phases present in the prepared solid materials. Further, the high-resolution XRD (HR-XRD) pattern probed the material's characteristic peak, indicating whether the dopant has occupied an interstitial position or substituted the corresponding cation or the anion. The UV-visible diffuse reflectance spectroscopy (UV-DRS) recorded the reflectance data of the synthesized samples. The Tauc plot derived from the UV-DRS data gave the photocatalysts bandgap. The transmission electron microscope (TEM) was used to capture the sizes and shapes of the prepared nanoparticles. High-resolution TEM (HR-TEM) imaging helped to photograph the crystalline fringes. The d-spacing between two fringes (also represents the lattice d-spacing) identified the presence of a particular phase. Photoluminescence (PL) studies were performed to measure the fluorescence intensities of the solid samples. The elements present, their oxidation states, and the defects in the materials were all investigated using X-ray photoelectron spectroscopy (XPS). It also provides the constituent elements' binding energies. UV-visible spectroscopy was employed. The absorbance of reaction mixtures subjected to photocatalytic degradation was measured.

**2.4.1. Powder X-Ray Diffraction (XRD)**

XRD is an effective technique for determining solid-state phases, crystallite sizes, and other properties. It also provides the nanoparticles' crystalline structure (Patterson, 1939). Because the solid samples may be recovered after the analysis, it is a non-destructive method. All powder XRD patterns were recorded using a Rigaku Miniflex 600 Desktop (RIGAKU Corporation, Japan) instrument. The instrument was equipped with a Cu K $\alpha$  irradiation source (The scan rate and step size for pattern collecting were 5° per minute and 0.01). The 2 $\theta$  angle was kept between 10° and 70°. To identify the phases generated, the XRD peaks were matched with typical XRD patterns (JCPDS database). Following Bragg's equation was used to obtain the lattice parameter (Pope, 1997).

$$n\lambda = 2d \sin\theta \text{ ----- (2.1)}$$

Where n represents the order of reflection,  $\lambda$  is the wavelength of incident X-ray radiation, and  $\theta$  is the Bragg angle between the incident light and the crystallographic plane.

**2.4.2. Sample preparation and imaging for Transmission Electron Microscopy (TEM)**

The TEM technique is extremely useful for imaging at the nanoscale. Furthermore, the high-resolution images provide structural information on the different crystalline phases (Smith, 2015). It can also determine the shapes and sizes of nanoparticles. For TEM sample preparation, a standard procedure was used in this thesis. First, the nanoparticles (from the sample) were dispersed in ethanol using suitable sonication and dilution. The redispersed sample was then transferred to the TEM grid (Cu grid with 400 mesh size). The sample grid was dried overnight in a 50°C oven. The constructed TEM sample grid was analysed using a Technai G2 20 TWIN (EDAX Inc.) instrument and a 200 kV accelerating voltage. The images were gathered from the grid's various

regions. The image depicts particle forms and average particle sizes. Image J software was used to calculate the average particle sizes and fringe spacing.

### **2.4.3. UV-Visible spectroscopy**

UV-visible absorption spectroscopy is a method of measuring light absorbance in the ultraviolet (UV) and visible parts of the electromagnetic spectrum. When light passes through the sample solution, it can be absorbed, transmitted, and reflected. Light absorption photo-excites electrons in a molecule via  $n \rightarrow \pi^*$ ,  $\pi \rightarrow \pi^*$ ,  $n \rightarrow \sigma^*$  electronic excitations (where the symbols represent non-bonding orbital ( $n$ ), bonding -orbital ( $\pi$ ), antibonding -orbital ( $\pi^*$ ) or antibonding  $\sigma$ -orbital ( $\sigma^*$ )). The molecule's functional groups cause a specific absorption that is detected by a UV-vis detector and recorded as a UV-vis absorbance spectrum. All UV-visible spectra of the samples are generated by the Agilent Cary 60 spectrophotometer. The diluted sample solution was placed in the spectrometer's sample holder slot in a cuvette with a 1 cm route length. It should be noted that the solvent was utilised for baseline correction (Scaffardi et al., 2013).

### **2.4.4. UV-visible diffuse reflectance spectroscopy (UV- DRS)**

The UV-DRS was used to determine the bandgap of the photocatalysts that were synthesised. The reflectance spectra of materials were acquired using a Shimadzu UV-2600 spectrophotometer. The absorbance data was then calculated using the Kubelka-Munk method using the reflectance data (Yang & Kruse, 2004). The Tauc plots were constructed from the absorbance data using the following formula:

$$(\alpha h\nu)^{1/n} = h\nu - E_g \text{-----} (2.2)$$

equation (2.2) Here,  $\alpha$  is the molar absorption coefficient,  $E_g$ ,  $\nu$  and  $h$  are the bandgap and frequency of light of the material. The optical band gap ( $E_g$ ) value of the photocatalyst is given by the x-axis intercept of the tangent to the linear component of the plot ( $1/n$  vs.  $h$ ). The optical bandgap's nature is determined by the  $n$  value. The values of  $n$  for direct and indirect bandgap are  $1/2$  and  $2$ , respectively.

#### **2.4.5. X-ray photoelectron spectroscopy (XPS)**

XPS is a quantitative analytical technique for determining the chemical state of components in a substance. The photoelectric effect occurs when X-rays strike the substance. The expelled electrons have kinetic energies that are measured by a detector. These kinetic energies are used to calculate the binding energies. Notably, the binding energy of an element in a specific oxidation state is unique.

A standard methodology was followed for sample preparation for the XPS measurement. The powder sample was first dispersed in ethanol before being deposited onto a square-shaped tiny glass slide. After that, the treated glass slide was dried in a hot air oven at 50 °C overnight. XPS measurements were performed on the glass slide containing the sample thin film (Li et al., 2021). All XPS measurements were performed on the K-ALPHA XPS apparatus (Thermo Fisher Scientific). The experimental results for the VB and CB positions are supplied with the NHE scale (valence band XPS (VBXPS)).

#### **2.4.6. Photoluminescence studies**

When light energy, or photons, promote the emission of a photon from any matter, it is called photoluminescence spectroscopy, or PL. It is a non-contact, non-destructive technique for material probing. In essence, a sample is exposed to light, which is absorbed there and can trigger a process known as photo-excitation. The material is moved to a higher electronic state by photo-excitation, and as it returns to its original lower energy level after relaxing, it releases energy (photons). Photoluminescence, or PL, is the process through which light or luminescence is emitted. In PL spectroscopy, UV radiation from a Xenon lamp at a wavelength of around 254 nm is allowed to fall on the material, which excites the electrons to a higher energy level. After losing energy, these extremely energetic electrons return to their ground state by emitting photons in the visible area, which the photomultiplier tube detects.

Because the PL signal often comes from the recombination of photogenerated electron-hole pairs, photoluminescence (PL) is utilised to analyse the separation of photogenerated charge carriers. To achieve effective photocatalytic performance, high PL intensity denotes greater charge carrier recombination, whereas low PL intensity denotes the maximum separation of charge carriers. The maximal charge carrier separation occurs in an ideal heterojunction, quenching the PL intensity. Additionally, the rate of charge carrier recombination is measured using the lifetime. For effective photocatalytic activity, a longer lifetime is crucial (Xu & Cotlet, 2013).

### **2.5. Photocatalytic performance measurements**

As a photocatalytic chamber, a constructed cube-shaped box was placed within one magnetic stirrer and bulb holder. As a source of visible light, a cool white LED bulb was used. The incoming light intensity was 1070 W/m<sup>2</sup>, as measured by a TM-206 power metre (pyrometer). In an ultrasonic bath, the photocatalyst sample nanoparticles were re-dispersed in an adequate volume of water. In a 4 ml quartz cuvette, the re-dispersed solution was combined with the organic molecule to be photo-catalytically degraded. An ultrasonic bath was used to properly distribute the resulting mixture. The mixture was then exposed to visible light irradiation. After a particular time, interval, the UV-visible absorption spectra were recorded. The photocatalytic experiments are described in full in Chapters 3, 4, 5, and 6. The catalysts' turnover frequency (TOF) values were also evaluated to determine the catalytic efficiency quantitatively. The procedure to determine TOF was identical to the photocatalytic trials. The following equation was used to calculate all the TOF values in the thesis.

$$TOF = \frac{\left[ \frac{\text{Number of moles of reactant}}{\text{Number of grams of catalyst}} \right] \times \text{Yield}}{\text{time}} \dots\dots\dots (2.3)$$

## **2.6. Scavenging experiments**

Separate photocatalytic experiments were also carried out with specific radical scavengers for determining the reactive species ( $\cdot\text{OH}$ ,  $\text{h}^+$  or  $\text{O}_2^{\cdot-}$ ) primarily responsible for degradation. The amounts of PBQ, or KI, or IPA used in different active species trapping experiments was 200 $\mu\text{l}$  (0.185 $\mu\text{M}$ ). Except for the added radical scavenger, the rest of the experimental conditions remained the same. Thus, isopropyl alcohol (IPA) was used as the scavenger for  $\cdot\text{OH}$  radicals, KI as a hole ( $\text{h}^+$ ) scavenger, and p-benzoquinone (PBQ) for removing superoxide radicals. Degradation efficiency was calculated and compared with a blank experiment (in the absence of a scavenger) (Kumar et al., 2019).